

Homeoprotein Hbx4 represses adhesion molecule governing cytokinesis and development

Ji-Sun Kim, Ji-Hui Seo, Hyung-Soon Yim & Sa-Ouk Kang

Laboratory of Biophysics, School of Biological Sciences, and Institute of Microbiology,
Seoul National University, Seoul 151-742, Republic of Korea

Homeobox genes encode proteins with a highly conserved DNA-binding motif and provoke morphological diversification of body segments by differentially controlling the expression of downstream targets. Here, we have identified *hb_x4*, one of many homeobox genes in *Dictyostelium discoideum* and investigated its role during growth and development. In suspension, Hbx4-overexpressing cells, Hbx4^{OE}, showed defects in cytokinesis and growth rate. During development, Hbx4^{OE} and *hb_x4*-disrupting cells, *hb_x4*⁻ made differences in shape of mound and slug, cell-type proportioning from wild type KAx3 cells. These phenotypes were similar to those of mutant defective in *cadA* encoding Ca²⁺-dependent cell adhesion molecule so that we investigated the relationship between *hb_x4* and *cadA*. Overexpression of Hbx4 inhibited the expression of *cadA* and cAMP also failed to stimulate *cadA* in Hbx4^{OE}. Furthermore, gel mobility shift assay showed the promoter of *cadA* contained Hbx4-binding site, indicating Hbx4 negatively regulates the expression of *cadA*. Proteome analysis revealed that overexpression of Hbx4 repressed the *rdiA* and *abpB* encoding rho guanine nucleotide dissociation inhibitor1, RhoGDI1 and actin bundling protein 34, ABP34, respectively. And the overexpression of *cadA* in Hbx4^{OE} cells rescued the defects and increased mRNA level of *rdiA*, *abpB* and one of Rho GTPase, *rac1b*. These results suggested that Hbx4 can modulate cytokinesis, cell sorting and cell-type proportioning by repressing *cadA* that regulates GTPase-dependent signaling pathway.

Homeobox (Hox) genes encode proteins with a highly conserved helix-turn-helix DNA-binding motif, the homeodomain, and function as transcription factors by directly binding to DNA sequences in Hox response elements. Hox genes have been known as important regulator in body segment during differentiation and development after being identified homeotic mutation in body segment disorder in *Drosophila*. However, recent studies have also focused on the role as modulator in proliferation and cell cycle^{1,10}. Because of their role as important regulator in embryogenesis and cell cycle, many researchers have struggled to find out target genes of Hox transcription factor. Therefore, we investigated function and action mechanism of hox gene in *Dictyostelium discoideum*. There are 14 predicted hox genes with one duplicate on chromosome 2. *DdHbx-1* (*wariai*) and *DdHbx-2*⁹ of them were already reported. We identified the *hbz4* (DDB_G0272967), homeobox-containing gene 4, which encodes conserved homeodomain (Supplementary Fig. 1a) and prepared overexpression (*Hbx4*^{OE}) and disruption (*hbz4*⁻) mutants. During development of wild-type KAx3 cells, mRNA level of *hbz4* increased gradually and maximum peak in 22 h (Supplementary Fig. 1b) suggesting Hbx4 may be involved in development.

As developed, *Hbx4*^{OE} cells showed severe aberrant morphological structures in mound, slug migration (Supplementary Fig. 2) and fruiting body (Fig. 1a). The *Hbx4*^{OE} cells formed large loose aggregates, which did not enter tight aggregate stage (Fig. 1a). And a large aggregate was separated into many small aggregates, which became tips and fruiting bodies independently. Furthermore, they became short and stubby slug, which is made of almost prestalk cells (Fig. 1b). And fruiting body of *Hbx4*^{OE} was composed with short stalk (Fig. 1b), clear sporeless-sorus (Fig. 1a) and huge basal disc consisted of rearguard and pstB cells, which could not participate in fruiting body and anterior-like cells (Fig. 1b). To determine whether Hbx4 is involved in cell-type proportioning, northern blot analysis was performed. In *Hbx4*^{OE} cells, prespore/spore-specific genes were not expressed at all while expressions of

prestalk genes increased (Fig. 1c), which is consistent with the morphological analysis. In contrast, *hbx4*⁻ slug was composed with increased prespore and decreased prestalk cells but they were able to produce mature fruiting bodies which have spores (Fig. 1a, b). Taken together, Hbx4 may regulate the sorting of prespore and prestalk cells, or the signal transduction pathway regulating prespore/prestalk differentiation directly or indirectly.

In suspension culture, we observed that single cells of Hbx4^{OE} were larger and grew slower than KAx3. To address the possibility that this phenomenon results from cytokinesis defect, we performed co-immunostaining with DAPI for DNA and TRITC-phalloidin for F-actin as described in method. In suspension, Hbx4^{OE} cells produced large multinucleate cells and *hbx4*⁻ cells showed mono- or dinucleate similar to KAx3 (Fig. 2a). The distribution of F-actin was also polarized in KAx3 and *hbx4*⁻ cells cortex, but it was depolarized in Hbx4^{OE} cells (Fig. 2a). Moreover, the rate of increase in cell number was significantly lower in Hbx4^{OE} cells and slightly higher in *hbx4*⁻ cells than that of KAx3 cells (Supplementary Fig. 4a) while the rates of increase in cell mass monitored as the turbidity of the culture were similar in KAx3, Hbx4^{OE} and *hbx4*⁻ cells (Supplementary Fig. 4b). And mutants exhibited different distributions of nuclei/cell depending on cell adhesion to solid substrate. In suspension, only 7.14% of Hbx4^{OE} cells were mononucleates and 38.1% of them became multinucleates which have more than four nuclei (Supplementary Fig. 5a), whereas when cultured on solid substrate, 92.22% of Hbx4^{OE} cells were mononucleates (Supplementary Fig. 5b), which is similar to the cytokinesis of mutants lacking myosin II^{4,14}. But the expression level of myosin II in Hbx4^{OE} cells was not changed (data not shown), suggesting that Hbx4 negatively regulates cytokinesis, in which another factor(s) rather than myosin II can be involved.

To gain insight into the mechanism underlying the distinctive defects of Hbx4 mutant cells, we examined the relationship between Hbx4 and DdCAD-1, which is important EDTA-

sensitive adhesion molecule during initial development⁷ since phenotype of *cadA* null cells is very similar to Hbx4^{OE} cells^{22,26,27} and gene expression profile of Hbx4^{OE} showed markedly reduced *cadA* expression (Fig. 1c). Western blot analysis showed that DdCAD-1 was not nearly expressed in Hbx4^{OE} cells and increased -1.5 fold in *hbx4*⁻ cells compared with KAx3 (Fig. 1d). Cohesion assay was also performed to assess the effects of lower DdCAD-1 expression on cell-cell adhesion caused by Hbx4 overexpression. In spite of the absence of chelator, reassociation of Hbx4^{OE} cells was significantly diminished by 75% in comparison with KAx3 (Supplementary Fig. 6a). These findings indicate that the overexpression of Hbx4 downregulates *cadA* expression and diminishes biological activity of DdCAD-1. It has been known that *cadA* expression is stimulated by cAMP pulses via G protein-dependent pathway²⁷. However, in Hbx4^{OE} cells *cadA* was not induced, even though *Gα* subunit (*gpaB*) was activated by cAMP (Fig. 1e) implying Hbx4 may interrupt the induction of *cadA*. The result of electrophoretic mobility shift assay with recombinant Hbx4 revealed *cadA* promoter contained Hbx4 binding site(s) (Supplementary Fig. 6b), which can explain how Hbx4 modulates *cadA* expression. To corroborate the relationship between Hbx4 and DdCAD-1, we overexpressed DdCAD-1 in KAx3 and Hbx4^{OE} cells. In Hbx4^{OE} cells, cytokinesis defect was recovered markedly by DdCAD-1 overexpression (CAD1^{OE}/Hbx4^{OE}, Fig. 2a and Supplementary Fig. 5) and abnormal morphology was partially rescued (Fig. 1a and Supplementary Fig. 3). Taken together, it is suggested that the homeoprotein Hbx4 may function as transcriptional regulator of DdCAD-1 to affect cytokinesis and development in *D. discoideum*.

To obtain a more precise view of regulatory mechanism by Hbx4 and DdCAD-1 in cytokinesis, proteomic analysis of KAx3 and Hbx4^{OE} cells was performed (Supplementary Fig. 7). RhoGDI1 (Rho GDP dissociation inhibitor1) and ABP34 (34 kD-actin bundling protein) were reduced in Hbx4^{OE} cells compared with KAx3. Furthermore, *rdiA* and *abpB*

encoding RhoGDI1 and ABP34^{15,16}, respectively, were derepressed by DdCAD-1 overexpression (Fig. 2b). And we observed that constitutively expressed RhoGDI1 also induces *abpB* (Fig. 2e) and most of induced *abpB* were localized in cortex of dividing cells, which coincide with the localization of F-actin (Supplementary Fig. 8). During development, the expressions of *rdiA* and *abpB* were also regulated by Hbx4 (data not shown). This result indicates that ABP34 can be a cytoskeleton protein involved in defective cytokinesis of Hbx4^{OE} cells instead of myosin II. In *Dictyostelium*, it has been reported that RhoGDI1-null cells showed defects in cytokinesis^{11,17} and actin cytoskeleton, which is consistent with the phenotype of Hbx4^{OE} that has repressed expression level of RhoGDI1. RhoGDI1 is able to interact with several RhoGTPases such as Rac1a/b/c, RacB, RacC and RacE¹¹ that can relay upstream signals to cytoskeletal components¹⁸. Therefore, we examined the effects of Hbx4 and DdCAD-1 on the expression of RhoGTPase. Transcription level of *rac1b* among several RhoGTPases was reduced in Hbx4^{OE} and increased by overexpression of DdCAD-1 (Fig. 2c) or RhoGDI1 (Fig. 2d), while there was no difference in the level of *rac1a* and *rac1c* in mutant strains (data not shown). Interestingly, RhoGDI1 elicits expression of *rac1b* specifically because RhoGDI is generally known to inhibit RhoGTPase⁶ and Rac1a/b/c have very high similarity in amino acid sequences. This finding suggests that Rac1b regulated by RhoGDI1 affects downstream genes including *abpB* (Fig. 3) leading to defective cytokinesis.

In this study, we demonstrated how homeodomain protein, Hbx4 regulates not only cell proportioning during development but cytokinesis. So far only a few reports represented the functions of homeoprotein in cytokinesis⁸ and there is no description about how homeoprotein affects cytokinesis⁵. Our experiments revealed that Hbx4 participates in signal-transduction processes governing cytokinesis through adhesion molecule and small GTPase. Therefore, we expect our findings can expand research area of hox genes.

Cell adhesion molecules have a mechanical function and may also regulate signal transduction cascade governing morphogenesis^{12,13}. DdCAD-1 and cadherins, a major class of adhesion molecules, share significant similarities in deduced amino acid sequence and Ca²⁺-binding motif in carboxy-terminal region^{3,25}, except that DdCAD-1 lacks transmembrane domain^{21,23}. So far, DdCAD-1 is known to be involved mainly in adhesion and regulated by Ras protein^{19,20}, but the investigation into Hbx4^{OE} and CAD1^{OE}/Hbx4^{OE} illustrates a novel role of DdCAD-1 as signal trigger that regulates GTPase like cadherins. And RhoGDI1-mediated Rac1b activation in DdCAD-1 signaling may provide an important clue about the mechanism that cell adhesion molecules modulate RhoGTPase activity². Therefore, the results shown above provide new and unexpected insights into the relationship between homeodomain protein and cytokinesis, between homeodomain protein and cell-cell adhesion molecule and between cell-cell adhesion molecule and RhoGTPase in *D. discoideum*.

METHODS SUMMARY

***Dictyostelium* cell culture and strain construction.** The details of cell culture and strain construction can be found in the Supplementary Information.

Real-time RT-PCR. Each RNA sample ($50 \text{ ng } \mu\text{l}^{-1}$) was reverse transcribed into cDNA by use of superscript III reverse transcriptase kit (Promega). Real-time PCR was carried out in $20 \mu\text{l}$ volumes by use of 96-well reaction plates (Bioplastics). Each PCR was performed with SYBR Premix Ex Taq (TaKaRa) and *mna* as endogenous control gene. Fluorescence was detected on an Applied Biosystems 7500 real-time PCR system. The real-time RT-PCR samples for each gene at each time point were done in triplicate, and cycle threshold values generated from the reactions were averaged. Cycle threshold values of each gene were normalized to the endogenous controls and calibrated to an average expression level for the gene being analyzed.

Fluorescence microscopy. Log-phase cells grown in suspension were diluted to 2.5×10^6 cells ml^{-1} with HL5 and fixed immediately (suspension) or transferred to slide glass and fixed after 3 days (surface). Fixing was performed with 1% formaldehyde in methanol at $-10 \text{ }^\circ\text{C}$ for 5 min and air-dried^{11,24}. For staining F-actin, cells were incubated with $3 \mu\text{g ml}^{-1}$ TRITC-phalloidin (Sigma) for 1 h and washed three times with PBS. And then cells were stained with $0.1 \mu\text{g ml}^{-1}$ DAPI (Sigma) and observed under a fluorescent microscope.

Full Methods and any associated references are available in the online version of the paper at www.nature.com/nature.

References

1. Andrezzaoli, M. *et al.* *Xrx1* controls proliferation and neurogenesis in *Xenopus* anterior neural plate. *Development* **130**, 5143-5154 (2003).
2. Arthur, W. T., Noren, N. K. & Burrige, K. Regulation of Rho family GTPases by cell-cell and cell-matrix adhesion. *Biol. Res.* **35**, 239-246 (2002).
3. Brar, S. K. & Siu, C. H. Characterization of the cell adhesion molecule gp24 in *Dictyostelium discoideum*. Mediation of cell-cell adhesion via a Ca²⁺-dependent mechanism. *J. Biol. Chem.* **268**, 24902-24909 (1993).
4. De Lozanne, A. & Spudich, J. A. Disruption of the *Dictyostelium* myosin heavy chain gene by homologous recombination. *Science* **236**, 1086-1091 (1987).
5. Del Bene, F. & Wittbrodt, J. Cell cycle control by homeobox genes in development and disease. *Semin. Cell Dev. Biol.* **16**, 449-460 (2005).
6. DerMardirossian, C. & Bokoch, G. M. GDIs: central regulatory molecules in Rho GTPase activation. *Trends Cell Biol.* **15**, 356-363 (2005).
7. Devreotes, P. Cell-cell interactions in *Dictyostelium* development. *Trends Genet.* **5**, 242-245 (1989).
8. Greenstein, D. *et al.* Targeted mutations in the *Caenorhabditis elegans* POU homeo box gene *ceh-18* cause defects in oocyte cell cycle arrest, gonad migration, and epidermal differentiation. *Genes. Dev.* **8**, 1935-1948 (1994).
9. Han, Z. & Firtel, R. A. The homeobox-containing gene *Wariai* regulates anterior-posterior patterning and cell-type homeostasis in *Dictyostelium*. *Development* **125**, 313-325 (1998).
10. Hu, G. *et al.* Msx homeobox genes inhibit differentiation through upregulation of *cyclin D1*. *Development* **128**, 2373-2384 (2001).

11. Imai, K. *et al.* A Rho GDP-dissociation inhibitor is involved in cytokinesis of *Dictyostelium*. *Biochem. Biophys. Res. Commun.* **296**, 305-312 (2002).
12. Juliano, R. L. Signal transduction by cell adhesion receptors and the cytoskeleton: functions of integrins, cadherins, selectins, and immunoglobulin-superfamily members. *Annu. Rev. Pharmacol. Toxicol.* **42**, 283-323 (2002).
13. Kibler, K. *et al.* A cell-adhesion pathway regulates intercellular communication during *Dictyostelium* development. *Dev. Biol.* **264**, 506-521 (2003).
14. Nagasaki, A., de Hostos, E. L. & Uyeda, T. Q. Genetic and morphological evidence for two parallel pathways of cell-cycle-coupled cytokinesis in *Dictyostelium*. *J. Cell Sci.* **115**, 2241-2251 (2002).
15. Pikzack, C. *et al.* Role of calcium-dependent actin-bundling proteins: characterization of *Dictyostelium* mutants lacking fimbrin and the 34-kilodalton protein. *Cell Motil. Cytoskeleton* **62**, 210-231 (2005).
16. Rivero, F., Furukawa, R., Fechheimer, M. & Noegel, A. A. Three actin cross-linking proteins, the 34 kDa actin-bundling protein, alpha-actinin and gelation factor (ABP-120), have both unique and redundant roles in the growth and development of *Dictyostelium*. *J. Cell Sci.* **112**, 2737-2751 (1999).
17. Rivero, F. *et al.* Defects in cytokinesis, actin reorganization and the contractile vacuole in cells deficient in RhoGDI. *EMBO J.* **21**, 4539-4549 (2002).
18. Rivero, F. & Somesh, B. P. Signal transduction pathways regulated by Rho GTPases in *Dictyostelium*. *J. Muscle Res. Cell Motil.* **23**, 737-749 (2002).
19. Secko, D. M., Insall, R. H., Spiegelman, G. B. & Weeks, G. The identification of *Dictyostelium* phosphoproteins altered in response to the activation of RasG. *Proteomics* **4**, 2629-2639 (2004).
20. Secko, D. M., Siu, C. H., Spiegelman, G. B. & Weeks, G. An activated Ras

protein alters cell adhesion by dephosphorylating *Dictyostelium* DdCAD-1.

Microbiology **152**, 1497-1505 (2006).

21. Sesaki, H. & Siu, C. H. Novel redistribution of the Ca²⁺-dependent cell adhesion molecule DdCAD-1 during development of *Dictyostelium discoideum*. *Dev. Biol.* **177**, 504-516 (1996).
22. Siu, C. H., Harris, T. J., Wang, J. & Wong, E. Regulation of cell-cell adhesion during *Dictyostelium* development. *Semin. Cell Dev. Biol.* **15**, 633-641 (2004).
23. Sriskanthadevan, S. *et al.* The cell adhesion Molecule DdCAD-1 is imported into contractile vacuoles by membrane invagination in a Ca²⁺- and conformation-dependent manner. *J. Biol. Chem.* **284**, 36377-36386 (2009).
24. Sutherland, B. W., Spiegelman, G. B. & Weeks, G. A Ras subfamily GTPase shows cell cycle-dependent nuclear localization. *EMBO Rep.* **2**, 1024-1028 (2001).
25. Wong, E. F. *et al.* Molecular cloning and characterization of DdCAD-1, a Ca²⁺-dependent cell-cell adhesion molecule, in *Dictyostelium discoideum*. *J. Biol. Chem.* **271**, 16399-16408 (1996).
26. Wong, E. *et al.* Disruption of the gene encoding the cell adhesion molecule DdCAD-1 leads to aberrant cell sorting and cell-type proportioning during *Dictyostelium* development. *Development* **129**, 3839-3850 (2002).
27. Yang, C., Brar, S. K., Desbarats, L. & Siu, C. H. Synthesis of the Ca²⁺-dependent cell adhesion molecule DdCAD-1 is regulated by multiple factors during *Dictyostelium* development. *Differentiation* **61**, 275-284 (1997).

Supplementary Information is linked to the online version of the paper at

www.nature.com/nature.

Acknowledgements We thank Dr. R. A. Firtel for providing the EXP4(+) and pA15Gal vectors, Dr. J. G. Williams for providing the pspAGal expression vectors, and Dr. C. H. Siu for providing the anti-DdCAD-1 antiserum, and Dr. Chang-Hoon Lee for providing a preliminary experimental result. This work was supported by the Korea Research Foundation Grant funded by the Korean Government (MOEHRD, Basic Research Promotion Fund) (KRF-2007–341-C00261). This work was also supported by the Research Fellowship of BK21 project.

Author Contributions S.-O. K. planned the project. J.-S. K. performed most of the experiments. J.-H. S. conducted experiments, particularly for Fig. 1e. J.-S. K., H.-S. Y. and S.-O. K. performed data analysis. S.-O. K. supervised all aspects of the project. All authors discussed the results and commented on the manuscript.

Author Information Reprints and permissions information is available at www.nature.com/reprints. Correspondence and requests for materials should be addressed to S.-O. K. (kangsaou@snu.ac.kr).

Figure legends

Figure 1 | Developmental phenotype and changes of expression of DdCAD-1 in KAx3 and Hbx4 mutants ($Hbx4^{OE}$ and $hbx4^-$) cells on non-nutrient agar plates.

a, Phenotype of KAx3, Hbx4 mutant cells developed on non-nutrient agar plates. Upper panels; aggregate. The bar represents 0.5 mm. Middle panels; sorus of KAx3 and Hbx4 mutant cells. *Dictyostelium discoideum* cells were developed on 1.5% KK2 plate under overhead light and photographed after 30 h. The bar represents 0.5 mm. Lower panels; Spore viability assay. Spores of KAx3 and Hbx4 mutant cells were collected. Then spores were treated with detergent 0.3% Triton X-100 for 10 min. Spore coat protein-specific staining calcofluor-fluorescence dye was treated to spores. Upper row of spore figures; spores did not treated with Triton X-100. Middle row of spore figures; spores treated with Triton X-100 were stained. Lower row of spore figures; merged image. The bar represents 6 μ m. **b**, Abberant cell sorting patterns in KAx3 and Hbx4 mutant cells. Upper panels; β -gal histochemical analysis of spatial patterning of prestalk in KAx3, $Hbx4^{OE}$ and $hbx4^-$ cells. Cells were transformed with either the complete *ecmA*O/*lacZ* promoter construct. *ecmA*O is expressed in the anterior prestalk domain including *pstAB*, *pstA* and *pstO* compartments. The arrowhead points to the anterior prestalk region. In $Hbx4^{OE}$ cells, some *ecmA*O/*lacZ*-expressing cells can be seen in the prespore domain and greater than in KAx3 cells. And in $hbx4^-$ cells, *ecmA*O/*lacZ*-expressing cells can be seen smaller than in KAx3 cells. Slugs are not all the same size. No difference in spatial patterning was observed between large and small slugs. The arrows indicate the anterior prestalk region of the slugs. The bar represents 0.4 mm. Lower panels; neutral red staining of *pstA* domain in KAx3 and Hbx4 mutant cells. Upper row of

neutral red staining; slug. Lower row of neutral red staining; fruiting body. The bar represents 0.4 mm. **c**, Developmental gene expression in KAx3 and Hbx4 mutant cells. KAx3, Hbx4^{OE} and *hbx4*⁻ cells were developed on non-nutrient agar plates and total RNA was extracted at the indicated times. Total RNA (20 µg) was blotted onto a nylon membrane, and analyzed on northern blots using fragments of the indicated genes as hybridization probes. *sp60/cotC* and *pspA*, prespore-specific; *spiA*, spore-specific; *cadA* and *csaA*, aggregation-specific; *lagC* post-aggregative genes; *ecmA* and *ecmB*, prestalk-specific; *rnlA* used as loading control. **d**, KAx3 and Hbx4^{OE} and *hbx4*⁻ cells were developed on KK2 agar plates and collected at different developmental stages. Western blot analysis was probed with anti-DdCAD-1 and anti-actin antisera. Equal amount of proteins was loaded from each sample. **e**, Effect of cAMP induction on *cadA* expression in KAx3 and Hbx4 mutant cells. Axenically grown cells were developed separately in KK2 buffer (pH 6.2) without or with cAMP pulse. Total RNA was isolated from cells at 0, 4 and 8 h during development and subjected to northern blot analysis probed with *cadA* and *gpaB*. *rnlA* used as loading control. -; without cAMP pulsing, +; with cAMP pulsing.

Figure 2 | Cytokinesis and regulation of *cadA*, *rdiA* and *abpB* in KAx3, Hbx4 mutant and DdCAD-1 double mutant cells (CAD1^{OE}/KAx3 and CAD1^{OE}/Hbx4^{OE}).

a, Double immunofluorescence staining with tetramethylrhodamine-5-(and 6)-isothiocyanate (TRITC)-conjugated phalloidin for staining of actin filaments and with 4',6-diamidino-2-phenylindole (DAPI) for staining of nuclei in cells grown in suspension or on glass surfaces. The bar represents 5 µm. **b**, Expression level of identified genes, *rdiA* and *abpB*, during growth in Hbx4 mutant and DdCAD-1 double mutant cells. Total RNA of log phase KAx3, Hbx4^{OE}, *hbx4*⁻, CAD1^{OE}/KAx3 and

CAD1^{OE}/Hbx4^{OE} cells were extracted during growth. And samples of total RNA (20 μ g) were analyzed on northern blots using fragments of the *rdiA* and *abpB* as hybridization probes. *mIA* used as loading control. **c**, Expression of *rac1b* gene during growth in KAx3 and Hbx4 mutant and DdCAD-1 double mutant cells. Total RNA was isolated from cells in growth stage and mRNA levels for *rac1b* were measured by real-time RT-PCR using a relative quantification protocol. **d**, Expression levels of *rac1a/b/c* genes during growth in KAx3 and RhoGDI1 overexpressing mutant (RhoGDI1^{OE}/KAx3) cells by real-time RT-PCR. **e**, Expression levels of *abpB* genes during growth in KAx3 and RhoGDI1^{OE}/KAx3 cells. All expression data were normalized by dividing the amount of target gene by the amount of *mIA* used as control. The values represent mean \pm s.d. of three independent experiments.

Figure 3 | Proposed model of the regulatory pathway by Hbx4 during growth and development in *D. discoideum*. Hbx4 regulates the expression level of *cadA*, which controls the *rdiA* and *abpB*. Hbx4 modulates the cytokinesis, actin cytoskeleton and cell type proportioning.

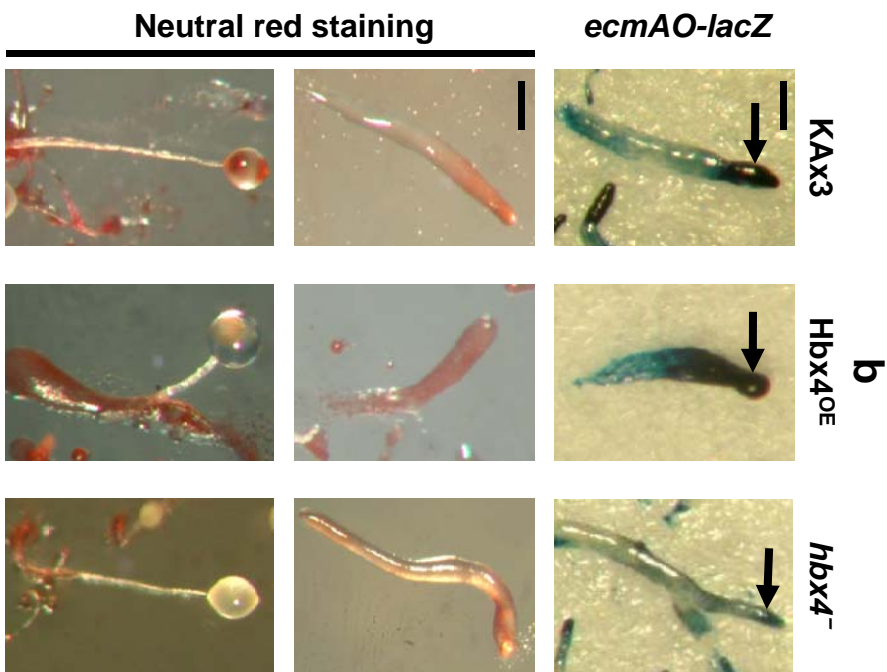
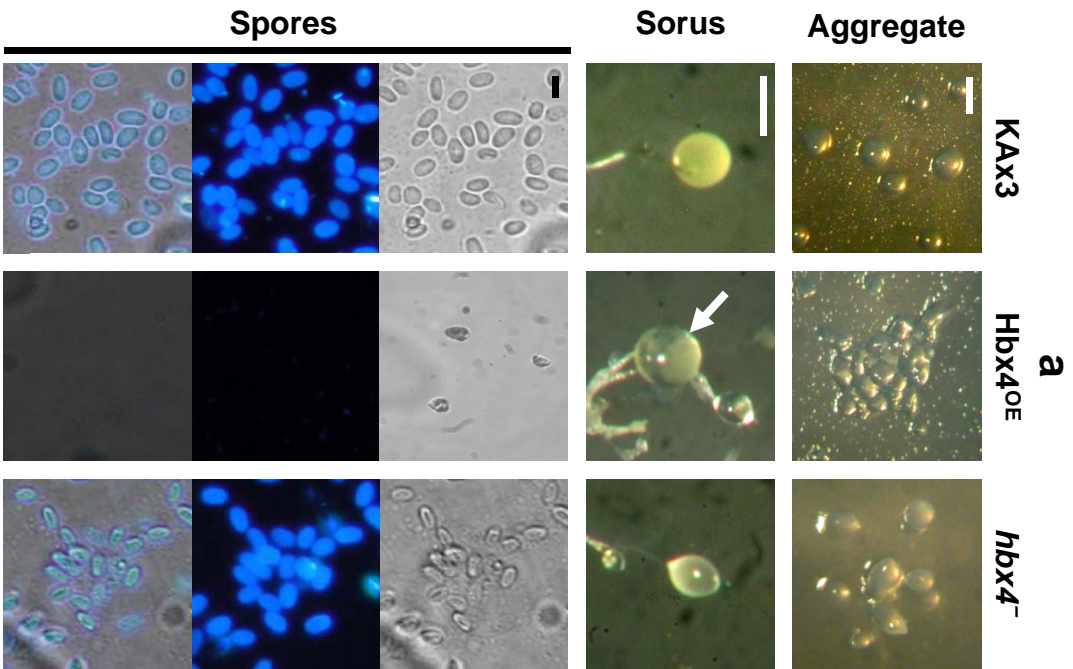


Figure 1

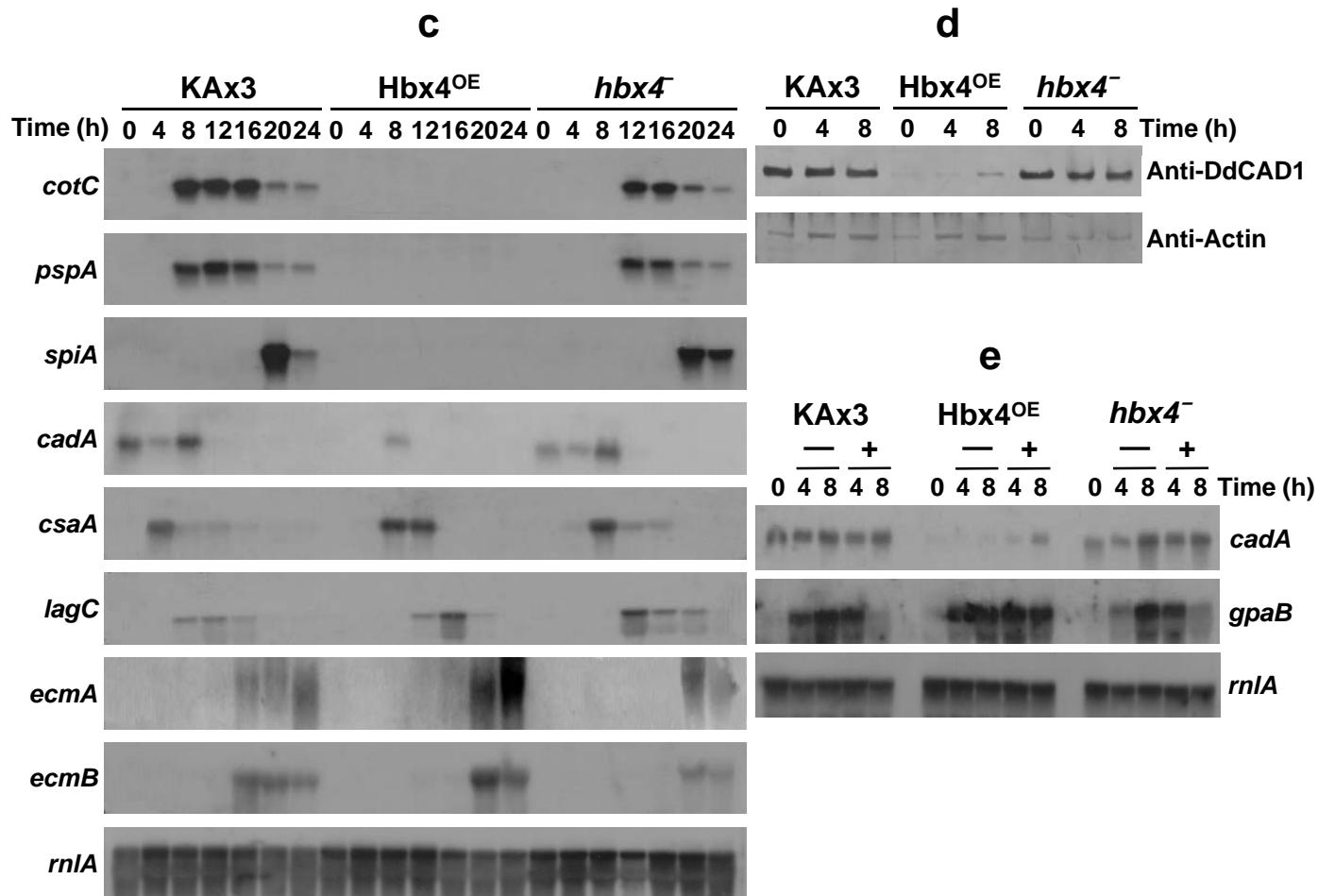


Figure 1

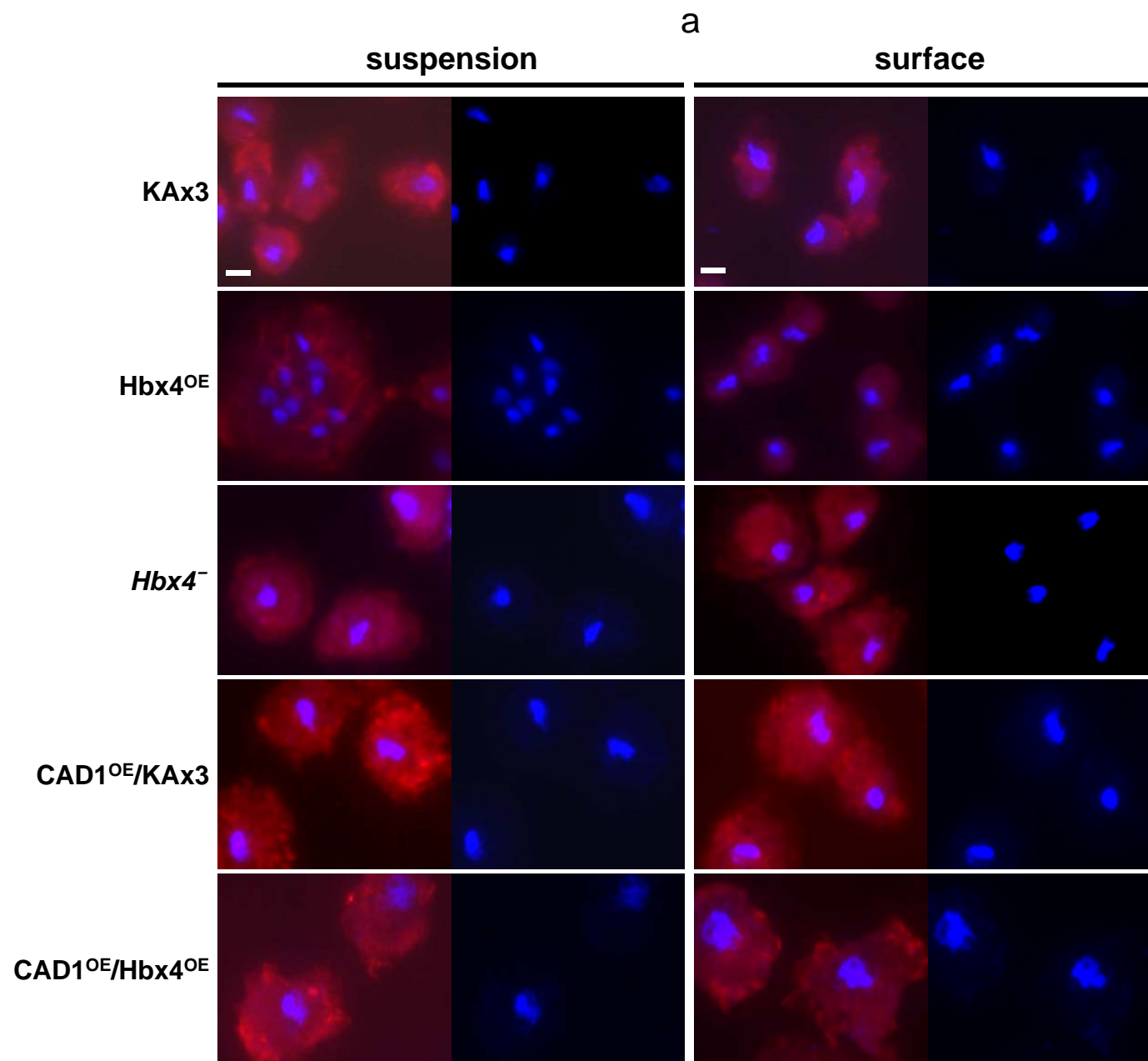


Figure 2

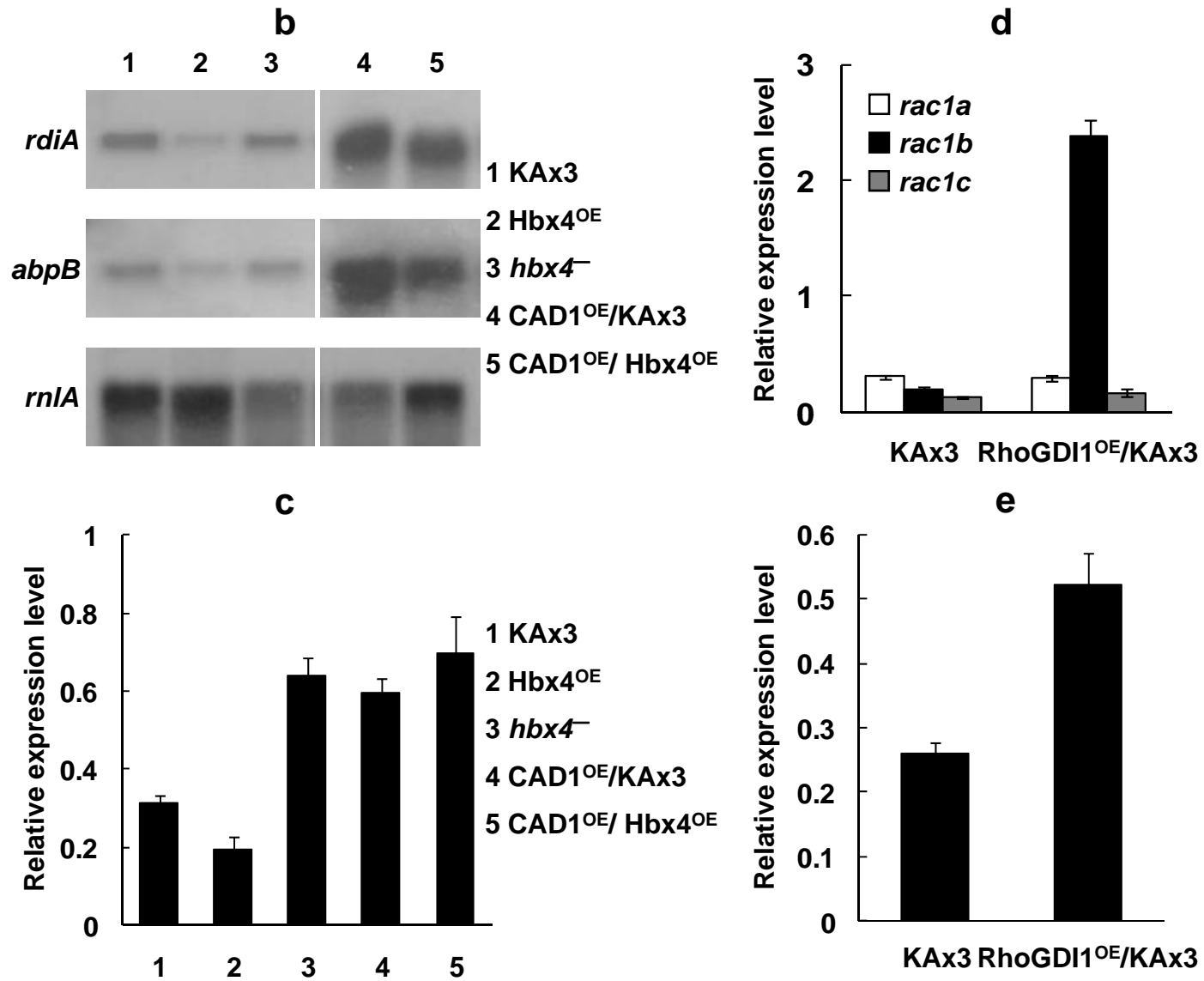


Figure 2

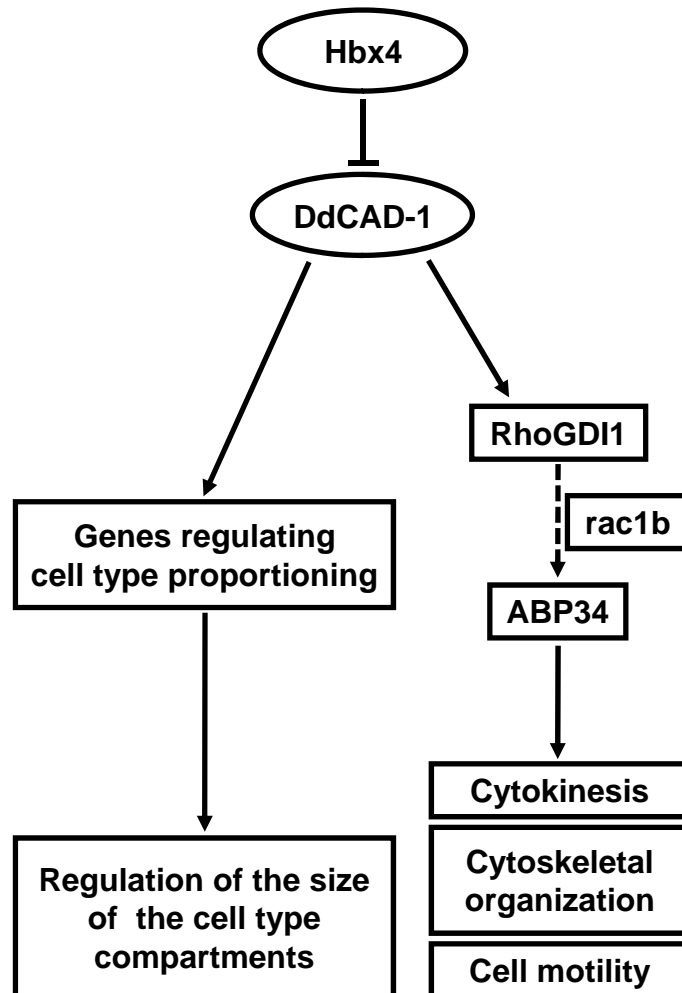


Figure 3